Article

# Probing the Location and Distribution of Paramagnetic Centers in Alkali Metal-Loaded Zeolites through Li MAS NMR

Victor V. Terskikh, Christopher I. Ratcliffe, John A. Ripmeester, Catherine J. Reinhold, Paul A. Anderson, and Peter P. Edwards

*J. Am. Chem. Soc.*, **2004**, 126 (36), 11350-11359• DOI: 10.1021/ja0491580 • Publication Date (Web): 20 August 2004

J|A|C|S
ARTICLES
Published on Web 08/20/2004

# Probing the Location and Distribution of Paramagnetic Centers in Alkali Metal-Loaded Zeolites through $^7$Li MAS NMR

Victor V. Terskikh,[†] Christopher I. Ratcliffe,*[,†] John A. Ripmeester,[†] Catherine J. Reinhold,[‡] Paul A. Anderson,*[,‡] and Peter P. Edwards*[,‡,||]

*Contribution from the Steacie Institute for Molecular Sciences, National Research Council of Canada, 100 Sussex Drive, Ottawa, Ontario, Canada, K1A 0R6, and School of Chemistry, The University of Birmingham, Edgbaston, Birmingham, U.K., B15 2TT*

Received February 16, 2004; E-mail: chris.ratcliffe@nrc-cnrc.gc.ca; p.a.anderson@bham.ac.uk; peter.edwards@chem.ox.ac.uk

***Abstract:*** The nature and surroundings of lithium cations in lithium-exchanged X and A zeolites following loading with the alkali metals Na, K, Rb, and Cs have been studied through $^7$Li solid-state NMR spectroscopy. It is demonstrated that the lithium in these zeolites is stable with respect to reduction by the other alkali metals. Even though the lithium cations are not directly involved in chemical interactions with the excess electrons introduced in the doping process, the corresponding $^7$Li NMR spectra are extremely sensitive to paramagnetic species that are located inside the zeolite cavities. This sensitivity makes $^7$Li NMR a useful probe to study the formation, distribution, and transformation of such species.

## Introduction

Dehydrated zeolites can absorb considerable amounts of alkali metals from the vapor phase to give brightly colored compounds, ranging from pink and green to dark blue, black, and even brown. First discovered almost 40 years ago,[1,2] these composite alkali metal−zeolite materials have become the subject of numerous studies because of the unique species and clusters which can form inside the zeolite voids.[3−5] Because the reaction with alkali metal vapor is usually carried out at reasonably low temperatures, the zeolites retain their crystallinity, and there is little if any destructive chemical reaction between the aluminosilicate zeolite framework and the alkali metal vapor. This preservation of the zeolite structure during reaction in many respects defines the unique properties of the resulting materials. The highly ordered one-, two-, or three-dimensional architecture of the zeolite voids (depending on the type of zeolite chosen) provides a natural template for the production and stabilization of low-dimensional metallic species and clusters of varying nuclearity, either paramagnetic or diamagnetic.

While the zeolite framework itself acts as a relatively inert porous template to accommodate such species, the charge-balancing cations, always present in the zeolites, are often involved in chemical interactions with the introduced alkali metal and can become an important constituent of the resulting clusters. For example, in potassium-loaded zeolite K−A both incoming $K^0$ atoms and charge balancing $K^+$ cations participate in cluster formation.[6,7] In Na−Y zeolite, $Na_4^{3+}$ clusters will form regardless of which doping alkali metal is used.[3a,b] Lighter alkali cations such as $Na^+$ and $K^+$ may be reduced by heavier alkali metals to form neutral atoms,[8] or even alkalide species, such as $Na^-$ in the K/Na−A[9] and Rb/Na−A[10,11] systems.

There are indications, however, that Li cations in Li-exchanged zeolites are much more resistant toward reduction.[12,13] In such systems, the incoming alkali metals do not appear to interact strongly with either the aluminosilicate framework, or the charge balancing cations, merely "dissolving" in the porous solid continuum. In effect, lithium cations may thus act as an "inert solvent", not reacting with the incoming guest, but enhancing the stability of the various species formed, some of which are quite unusual, such as the rubidide ion $Rb^-$, in Rb-loaded Li−A zeolite.[11] The concept of zeolites as solid

[†] National Research Council of Canada.
[‡] The University of Birmingham.
[||] Currently at the Inorganic Chemistry Laboratory, Oxford University.

(1) Rabo, J. A.; Angell, C. L.; Kasai, P. H.; Schomaker, V. *Discuss. Faraday Soc.* **1966**, *41*, 328.
(2) Barrer, R. M.; Cole, J. F. *J. Phys. Chem. Solids* **1968**, *29*, 1755.
(3) (a) Edwards, P. P.; Harrison, M. R.; Klinowski, J.; Ramdas, S.; Thomas, J. M.; Johnson, D. C.; Page, C. J. *J. Chem. Soc., Chem. Commun.* **1984**, 982. (b) Harrison, M. R.; Edwards, P. P.; Klinowski, J.; Thomas, J. M.; Johnson, D. C.; Page, C. J. *J. Solid State Chem.* **1984**, *54*, 330. (c) Anderson, P. A.; Edwards, P. P. *J. Chem. Soc., Chem. Commun.* **1991**, 915. (d) Anderson, P. A.; Singer, R. J.; Edwards, P. P. *J. Chem. Soc., Chem. Commun.* **1991**, 914. (e) Edwards, P. P.; Anderson, P. A.; Thomas, J. M. *Acc. Chem. Res.* **1996**, *29*, 23. (f) Woodall, L. J.; Anderson, P. A.; Armstrong, A. R.; Edwards, P. P. *J. Chem. Soc., Dalton Trans.* **1996**, 719.
(4) Ursenbach, C. P.; Madden, P. A.; Stich, I.; Payne, M. C. *J. Phys. Chem.* **1995**, *99*, 6697.
(5) Anderson, P. A. In *Molecular Sieves, Vol. 3, Postsynthesis Modification 1*; Karge, H. G., Weitkamp, J., Eds.; Springer-Verlag: Berlin & Heidelberg, 2002; Chapter 5, pp 307−338 and references therein.
(6) (a) Armstrong, A. R.; Anderson, P. A.; Edwards, P. P. *J. Chem. Soc., Chem. Commun.* **1994**, 473. (b) Armstrong, A. R.; Anderson, P. A.; Edwards, P. P. *J. Solid State Chem.* **1994**, *111*, 178.
(7) Ikeda, T.; Kodaira, T.; Izumi, F.; Kamiyama, T.; Ohshima, K. *Chem. Phys. Lett.* **2000**, *318*, 93.
(8) (a) Heo, N.-H.; Seff, K. *J. Chem. Soc., Chem. Commun.* **1987**, 1225. (b) Song, S. H.; Kim, U. S.; Kim, Y.; Seff, K. *J. Phys. Chem.* **1992**, *96*, 10937.
(9) Nakayama, H.; Klug, D. D.; Ratcliffe, C. I.; Ripmeester, J. A. *J. Am. Chem. Soc.* **1994**, *116*, 9777.
(10) Barker, P. D.; Anderson, P. A.; Dupree, R.; Kitchin, S.; Edwards, P. P.; Woodall, L. *J. Mater. Res. Soc. Symp. Proc.* **1996**, *431*, 191.
(11) Terskikh, V. V.; Moudrakovski, I. L.; Ratcliffe, C. I.; Ripmeester, J. A.; Reinhold, C. J.; Anderson, P. A.; Edwards, P. P. *J. Am. Chem. Soc.* **2001**, *123*, 2891.
(12) Anderson, P. A.; Barr, D.; Edwards, P. P. *Angew. Chem., Int. Ed. Engl.* **1991**, *30*, 1501.
(13) Xu, B.; Kevan, L. *J. Phys. Chem.* **1992**, *96*, 2642.


**10.1021/ja0491580 CCC: $27.50** 

solvents is well established in the field of catalysis, to describe different aspects of catalytic processes, involving high acidity and selectivity.[14] A close analogy has also been drawn between the dissolution of alkali metals in zeolites and solutions of alkali metals in liquid ammonia and other polar solvents.[3,5,15]

The positive identification of alkali metal clusters in zeolites has relied heavily on two types of experimental data.[5] First, ESR spectroscopy has been used to identify a large number of paramagnetic clusters, but can only do so when they are present in the zeolite in relatively low concentrations when electron spin−spin exchange interactions between the paramagnetic centers do not occur. Clearly, the technique is not applicable to diamagnetic species. Second, the averaging nature of diffraction methods, in contrast, has meant that these are effective in situations where clusters are present in relatively large numbers and are well ordered in the zeolite structure. Even in favorable cases, however, the degree of paramagnetism present is not readily available from diffraction studies. As a result of these limitations, it is fair to say that, despite the undoubted success of the two techniques, there are only a few alkali metal−zeolite systems where the complete range of paramagnetic and diamagnetic species present, and their distribution within the zeolite, is fully characterized.

In the present work, we have used $^{7}$Li solid-state NMR spectroscopy to probe the environment of lithium cations in lithium-exchanged X and A zeolites loaded to different extents with the alkali metals Na, K, Rb, and Cs. Solid-state NMR spectroscopy of lithium is established as a powerful and efficient technique to study a wide variety of Li-containing materials. Of the two lithium magnetic isotopes $^{6}$Li ($I = 1$, natural abundance 7.4%) and $^{7}$Li ($I = {}^{3}/_{2}$, natural abundance 92.6%), the latter is more commonly used, because no special isotopic enrichment is needed, although it has larger nuclear dipolar and quadrupolar moments than $^{6}$Li.

$^{6,7}$Li solid-state NMR spectroscopy has been applied successfully to Li-exchanged zeolites to locate and characterize crystallographically different intrapore Li sites.[16,17] One of the most practically important[18] was an investigation of the accessibility of Li cations in Li−X zeolite to gaseous oxygen and nitrogen, based on the acute sensitivity of $^{6,7}$Li NMR parameters to paramagnetic interactions (in that case with oxygen molecules).[19]

## Experimental Section

Zeolites Na−X ($Na_{89}[Al_{89}Si_{103}O_{384}]$, Si/Al = 1.16) and Na−A ($Na_{96}[Al_{96}Si_{96}O_{384}]$) were synthesized according to established procedures.[20] Crystallinity was confirmed by powder X-ray diffraction. Lithium-exchanged zeolites were prepared by ion exchange using a 1.0 M solution of $LiNO_3$ stirred overnight at 70 °C. The exchange process was repeated five times. According to chemical analysis (ICP-AES), exchange levels were about 95% in both cases, so that the compositions of the lithium-exchanged zeolites were $Li_{84}Na_5[Al_{89}Si_{103}O_{384}]$ (Li−X) and $Li_{90}Na_6[Al_{96}Si_{96}O_{384}]$ (Li−A). Samples loaded to various levels with alkali metals, $M_x$/Li−X and $M_x$/Li−A [$x$ = number of metal atoms per unit cell], were prepared with M = Na, K, Rb, and Cs. The samples were synthesized by dehydrating the ion-exchanged zeolite in a quartz tube under vacuum ($<10^{-5}$ Torr) at 400 °C for 12 h, loading with a known amount of alkali metal in an argon atmosphere glovebox, and then reevacuating the tube before sealing. The reaction tubes were heated at 200−300 °C until completion of the reaction (usually several days). For ESR experiments, the samples were sealed in evacuated Spectrosil quartz tubes. For NMR characterization, the samples were sealed under vacuum into 5 mm o.d. quartz tubes, sized to fit a stretched 7 mm Bruker MAS rotor ($ZrO_2$).

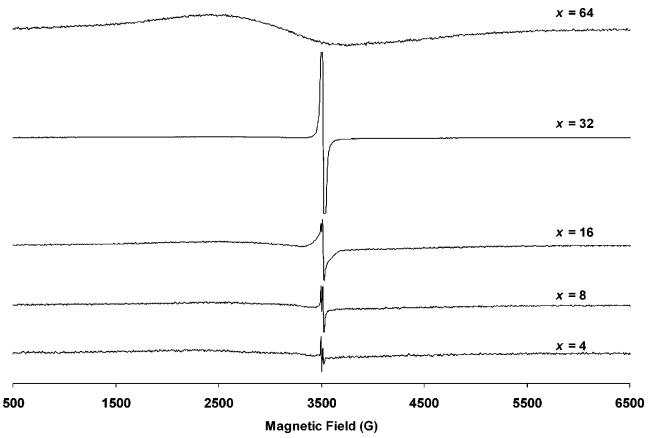


***Figure 1.*** ESR spectra of $Rb_x$/LiX ($x$ = 4, 8, 16, 32, 64 atoms per unit cell) at ambient temperature.

ESR spectra of all samples were recorded at room temperature on a Bruker ESP 300E spectrometer operating at X-band frequencies (~9.5 GHz) with 100 kHz field modulation and ESP 3220 data software. High-resolution solid-state $^{7}$Li MAS NMR spectra were recorded on a Bruker DSX-400 spectrometer, operating at a frequency of 155.5 MHz, with a Bruker 7 mm MAS probe at spinning frequencies of 3.5−4.0 kHz. Very short rf pulses of 0.6−1 $\mu$s (less than $\pi/12$) were applied in the single pulse experiments with relaxation delays of 1 s, which was sufficient for complete relaxation. The spectral sweep width was 400 kHz. The chemical shifts were referenced to a 1 M water solution of LiCl with an accuracy better than 0.1 ppm. Variable-temperature experiments were performed using a Bruker BVT-3000 temperature controller. Spectral deconvolution was performed using Bruker WIN-NMR software.

## Results and Discussion

**ESR Spectra.** The ESR spectra of all of the materials studied showed ample evidence of the presence of paramagnetic centers. An example is shown in Figure 1 for $Rb_x$/LiX as the loading of Rb is progressively doubled, with the corresponding parameters given in Table 1. A common feature of the ESR spectra recorded was a signal with a $g$-value characteristic of electrons associating with the incoming metal, sometimes accompanied by one or two additional resonances.[21] Hyperfine splitting was observed in only one case ($Na_{32}$/LiX) with a value characteristic of a sodium cluster. Unfortunately, the pattern was not sufficiently

(14) Derouane, E. G. *J. Mol. Catal. A* **1998**, *134*, 29.
(15) Thompson, J. C. *Electrons in Liquid Ammonia*; Oxford University Press: London and New York, 1976.
(16) (a) Schimiczek, B.; Greth, R.; Boddenberg, B. In *Zeolites and Related Microporous Materials: State of Art 1994, Studies in Surface Science and Catalysis*; Weitkamp, J., Karge, H. G., Pfeifer, H., Holderich, W., Eds.; Elsevier Science B. V.: New York, 1994; Vol. 84, p 733. (b) Feuerstein, M.; Engelhardt, G.; McDaniel, P. L.; MacDougall, J. E.; Gaffney, T. R. *Microporous Mesoporous Mater.* **1998**, *26*, 27. (c) Oka, H.; Kasahara, S.; Okada, T.; Yoshida, S.; Harada, A.; Ohki, H.; Okuda, T. *Microporous Mesoporous Mater.* **2002**, *51*, 1.
(17) Feuerstein, M.; Lobo, R. F. *Chem. Mater.* **1998**, *10*, 2179.
(18) Li−X zeolites are commercially used for the production of nitrogen from air in the pressure swing adsorption (PSA) process, see: (a) Gaffney, T. R. *Curr. Opin. Solid State Mater. Sci.* **1996**, *1*, 69. (b) Yang, R. T. *Gas Separation by Adsorption Processes*; Butterworth: Boston, 1987.
(19) (a) Feuerstein, M.; Lobo, R. F. *J. Chem. Soc., Chem. Commun.* **1998**, *16*, 1647. (b) Plévert, J.; de Ménorval, L. C.; Di Renzo, F.; Fajula, F. *J. Phys. Chem. B* **1998**, *102*, 3412. (c) Feuerstein, M.; Accardi, R. J.; Lobo, R. F. *J. Phys. Chem. B* **2000**, *104*, 10282. (d) Accardi, R. J.; Lobo, R. F. *Microporous Mesoporous Mater.* **2000**, *40*, 25.
(20) See the website http://www.iza-structure.org/ for the references.
(21) Reinhold, C. J. Ph.D. Thesis, The University of Birmingham, 2003.

***Table 1.*** ESR Parameters for $Rb_x$/LiX

| sample | temp (K) | *g*-value | $\Delta H_{pp}$ | spins per $cm^3$ (observed) | percentage spins[a] |
|---|---|---|---|---|---|
| $Rb_4$/LiX | 291 | 2.19 (±0.01) | 1500 (±50 G) | $1.76 \times 10^{20}$ | 66 |
| | | 2.0029 (±0.0001) | 4.6 (±0.2 G) | | |
| | | 1.9913 (±0.0001) | 10.1 (±0.2 G) | | |
| $Rb_8$/LiX | 291 | 2.14 (±0.01) | 1250 (±50 G) | $2.81 \times 10^{20}$ | 53 |
| | | 2.0029 (±0.0001) | 4.3 (±0.2 G) | | |
| | | 1.9915 (±0.0001) | 10.3 (±0.2 G) | | |
| $Rb_{16}$/LiX | 291 | 2.10 (±0.01) | 1350 (±50 G) | $4.63 \times 10^{20}$ | 44 |
| | | 2.0030 (±0.0001) | 4.4 (±0.2 G) | | |
| | | 1.9918 (±0.0001) | 13.3 (±0.2 G) | | |
| $Rb_{32}$/LiX | 291 | 1.9916 (±0.0001) | 12.2 (±0.2 G) | $8.79 \times 10^{20}$ | 41 |
| $Rb_{64}$/LiX | 291 | 2.18 (±0.01) | 1320 (±50 G) | $7.33 \times 10^{20}$ | 17 |
| | | 2.0022 (±0.0005) | 14 (±1 G) | | |

[a] ESR intensity as a percentage of that expected if each Rb 5s electron remained unpaired on reacting with the zeolite.

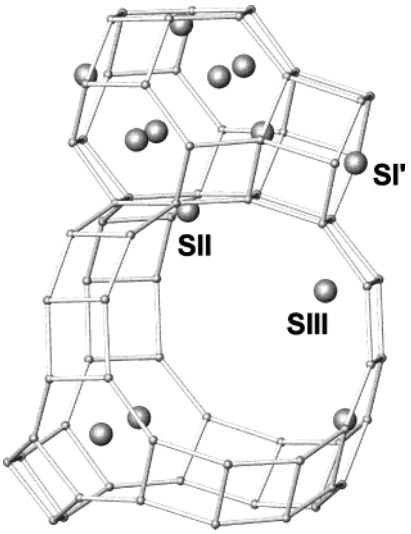


***Figure 2.*** Positions of Li cations in dehydrated zeolite Li−X at room temperature.[24]

well resolved to determine the nuclearity of the cluster, although the magnitude of the splitting suggests $Na_4^{3+}$. In general, however, it was not possible to identify specific paramagnetic species. The level of paramagnetism was substantial in all samples. In most cases, the spin count tends to decrease with metal loading due either to interactions or to the formation of diamagnetic clusters.

**Dehydrated Zeolite Li−X.** Zeolite X has a framework of the faujasite type (FAU)[22] consisting of small sodalite cages interconnected via hexagonal prisms in such a way that they define large tetrahedral supercages. Previous neutron diffraction studies of dehydrated Li−X have found $Li^+$ cations in three different crystallographic sites[23,24] shown in Figure 2: (a) In site SI′, the $Li^+$ is in a 6-ring window of the sodalite cage which is shared with the hexagonal prism, displaced slightly into the sodalite cage. There are 32 such sites per unit cell. (b) In site SII, the $Li^+$ is in a 6-ring window of the sodalite cage which is shared with the supercage, displaced slightly into the supercage. There are 32 such sites per unit cell. (c) In site SIII, the $Li^+$ is inside the supercage in front of those 4-rings which form part of the sodalite cage. There are 48 SIII sites per unit cell.

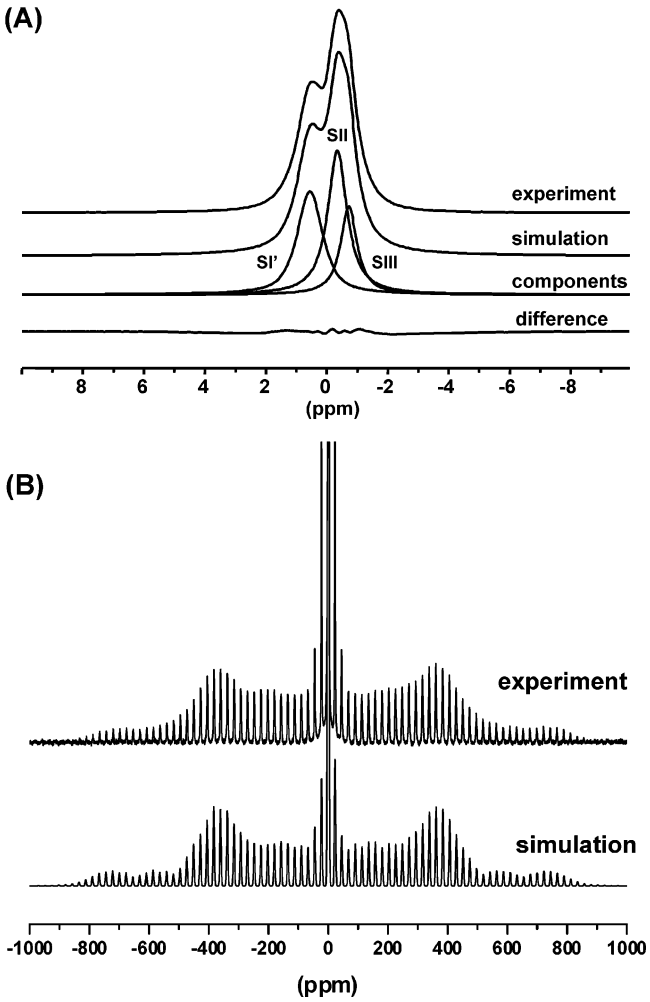


***Figure 3.*** $^7$Li MAS NMR (A) and SATRAS NMR (B) spectra of dehydrated Li−X zeolite ($\nu_o$ = 155.5 MHz, $\nu_{rot}$ = 3.5 kHz).

In agreement with the diffraction data, three distinct lines can be seen in the $^7$Li MAS NMR spectra of the dehydrated Li−X zeolite (Figure 3A). Assignment of the lines to the three crystallographic cationic sites was made following Feuerstein and Lobo.[17] Accordingly, the $Li^+$ at sites SI′, SII, and SIII have $^7$Li chemical shifts of 0.6, −0.4, and −0.7 ppm, respectively. Relative fractional occupancies of the different sites can be obtained from deconvolution of the $^7$Li NMR spectrum[25] and depend on the Si/Al ratio.

Sites SI′ and SII are energetically preferred and the first to be filled. Thus, for the Li−X material studied here, which has 84

(22) Baerlocher, Ch.; Meier, W. M.; Olson, D. H. *Atlas of Zeolite Framework Types*, 5th revised ed.; Elsevier: Amsterdam, 2001.
(23) Forano, C.; Slade, R. C.; Krogh Anderson, E.; Krogh Anderson, I. G.; Prince, E. J. *Solid State Chem.* **1989**, *82*, 95.
(24) Plévert, J.; Di Renzo, F.; Fajula, F.; Chiari, G. *J. Phys. Chem. B* **1997**, *101*, 10340.

***Table 2.*** Parameters for the Simulation of the $^7$Li MAS NMR Spectra of the Rubidium-Loaded Zeolite Li−X[25]

| sample | position | $\delta$, ppm ±0.05 | $\Delta\nu_{1/2}$, Hz ±10 | $I$, % ±3 |
|---|---|---|---|---|
| Li−X | SI′ | 0.55 | 155 | 37 |
| | SII | −0.35 | 120 | 41 |
| | SIII | −0.73 | 100 | 22 |
| $Rb_4$/Li−X | SI′ | 0.56 | 155 | 41 |
| | SII | −0.33 | 115 | 40 |
| | SIII | −0.67 | 100 | 19 |
| $Rb_8$/Li−X | SI′ | 0.57 | 150 | 44 |
| | SII | −0.32 | 115 | 40 |
| | SIII | −0.64 | 100 | 16 |
| $Rb_{12}$/Li−X | SI′ | 0.55 | 170 | 48 |
| | SII | −0.35 | 120 | 36 |
| | SIII | −0.70 | 110 | 16 |
| $Rb_{16}$/Li−X | SIII | 1.54 | 470 | 11 |
| | SI′ | 0.55 | 170 | 39 |
| | SII | −0.42 | 160 | 50 |
| $Rb_{24}$/Li−X | SIII | 15.6 | 1290 | 4 |
| | SII* | 1.56 | 280 | 30 |
| | SI′ | 0.57 | 280 | 51 |
| | SII | −0.32 | 150 | 15 |
| $Rb_{32}$/Li−X | SII* | 1.89 | 700 | 30 |
| | SI′ | 0.88 | 260 | 53 |
| | SII | −0.29 | 230 | 18 |
| $Rb_{64}$/Li−X | SII* | 3.65 | 1100 | 34 |
| | SI′ | 1.49 | 330 | 49 |
| | SII | −0.29 | 470 | 17 |

Li per unit cell, one might expect the distribution of $Li^+$ cations to be 32 SI′, 32 SII, and 20 SIII. This compares with 31.1:34.4:18.5, based on the relative integral intensities of the deconvolved lines (Table 2). The match between expected and observed is remarkably good and within experimental error. According to chemical analysis, some of the remaining SIII sites must be occupied by residual $Na^+$ cations (to the extent of 5 Na per unit cell), and this has also been confirmed by $^{23}$Na MAS NMR.[21]

All three sites have a nonspherical symmetry; therefore, all Li cations are influenced by quadrupolar interactions. However, the corresponding quadrupolar coupling constants ($C_Q$) are small enough[17] so that the second-order quadrupolar interaction has a negligible effect on the powder line shapes of the central transitions, Figure 3A. Information about the $C_Q$ and asymmetry parameters ($\eta$) was obtained from $^7$Li satellite transition MAS NMR (SATRAS)[26,27] spectroscopy. The spectrum for dehydrated Li−X is shown in Figure 3B. Analysis of the rotational spinning sidebands (ssb's) originating from the satellite transitions gives the $C_Q$ and $\eta$ parameters. In this spectrum, only the two sites SI′ and SII contribute to the ssb's, and these have very similar quadrupole coupling parameters, so that their ssb's closely overlap. The spectral simulation[28] shown in Figure 3B (bottom) was therefore calculated with a single set of parameters, $C_Q$ = 0.26 MHz and $\eta$ = 0.12, which agree well with the results reported previously.[17,29] The SIII site is quite asymmetric, and hence the $Li^+$ here would be expected to have a significant $C_Q$. However, due to dynamic exchange of the $Li^+$ cations among the SIII sites, the corresponding satellite ssb's are broadened beyond detection.[17] Consequently, only the central transition is observed. This fits with the observed integral intensities discussed above, because if $C_Q$ happened to be zero or very small the satellites and central transition for the SIII $Li^+$ would be superimposed, and the intensity would be 2.5 times higher. In this case, the expected SI′:SII:SIII ratio would be 32:32:50, which is definitely not the case. (The intensity ratios for the three transitions of a spin $^3/_2$ nucleus are 3:4:3, where 4 represents the central transition.)

**Rb-Loaded Zeolite Li−X.** A series of rubidium-loaded lithium-exchanged zeolite X samples ($Rb_x$/Li−X) was prepared, with $x$ = 4, 8, 12, 16, 24, 32, and 64 Rb atoms per unit cell. The effect of the Rb loading on the corresponding $^7$Li MAS NMR spectra (centerbands) is shown in Figure 4. Inserted in Figure 4A is an extended part of the spectrum for $Rb_{24}$/Li−X showing a broad line at 15.6 ppm (marked with an arrow). For all of the other samples, only spinning sidebands are observed outside the centerband region shown (−15 to +20 ppm). Detailed parameters from the spectral deconvolutions (chemical shifts, line widths, and relative integral intensities of the components) are given in Table 2. The number of components used in the deconvolutions was kept to a minimum,[25] taking as a basis the simulation for the dehydrated Li−X sample (Figure 3A), although for the broader spectra (at higher loadings) the simulations presented may not be unique. Examples of spectral simulations for highly loaded samples are shown in Figure 4B. Figure 5 summarizes graphically the chemical shifts of the different components as a function of the rubidium loading.

At loadings below 12 Rb atoms per unit cell, only subtle changes in the $^7$Li spectra can be seen: a gradual decrease in intensity of the SIII component (see Table 2), while the two major components of approximately equal integral intensities from sites SI′ and SII remain practically unchanged. In $Rb_{16}$/Li−X, the SIII $Li^+$ resonance, half-reduced in intensity relative to the starting Li−X and broadened, has moved more than 2 ppm downfield from its original position to 1.5 ppm, while the SI′ and SII $Li^+$ resonances are still largely unchanged. However, much more dramatic changes are visible in the spectrum of $Rb_{24}$/Li−X: (a) the SIII component is now at 15.6 ppm, with only one-quarter of its initial intensity, and 10 times broader than in the starting zeolite. (b) The line from SII cations is split into two components, of which one remains practically unchanged at −0.3 ppm, with roughly $^1/_3$ of the initial intensity, and the second is shifted to 1.6 ppm, with about $^2/_3$ of the initial intensity. (For clarity, the sites corresponding to this shifted line will now be labeled SII*.) (c) The SI′ line in this sample remains unchanged in its position or relative intensity, but there is some broadening. At still higher loadings ($Rb_{32}$/Li−X and $Rb_{64}$/Li−X): (a) the line from SIII cations is no longer observed, due to severe broadening and shifting out of the spectral window. (b) The broadening becomes greater for the SII component and quite severe for the SII* component, yet still only SII* is shifted downfield, while SII remains at −0.3 ppm. (c) The SI′ line is shifted slightly downfield with very moderate broadening. Assignment of the NMR lines to particular lithium sites is greatly facilitated by the fact that the relative intensity of the SI′ line remains practically unchanged during these transformations, being roughly equal to the relative intensity of the SII line before it splits and then to the sum of intensities of the

(25) Although most of the spectra were simulated with pure Lorentzian lines, in some cases a small fraction of the Gaussian shape (G/L = 0.3) was added to keep as few components in the simulation as possible.

(26) Jager C. Satellite Transition Spectroscopy of Quadrupolar Nuclei. *NMR Basic Principles and Progress*; Springer: New York, 1994; Vol. 31, p 133.
(27) Skibsted, J.; Nielsen, N. C.; Bildsoe, H.; Jacobsen, H. J. *J. Magn. Reson.* **1991**, *5*, 88.
(28) The SATRAS simulation software used in this work was developed by H. Ohki, see: Oka, H.; Tokunaga, Y.; Okada, T.; Ohki, H.; Okuda, T. *Microporous Mesoporous Mater.* **1999**, *33*, 257.
(29) Lechert, H.; Basler, W. D.; Henneke, H. W. *Ber. Bunsen-Ges. Phys. Chem.* **1975**, *79*, 563.

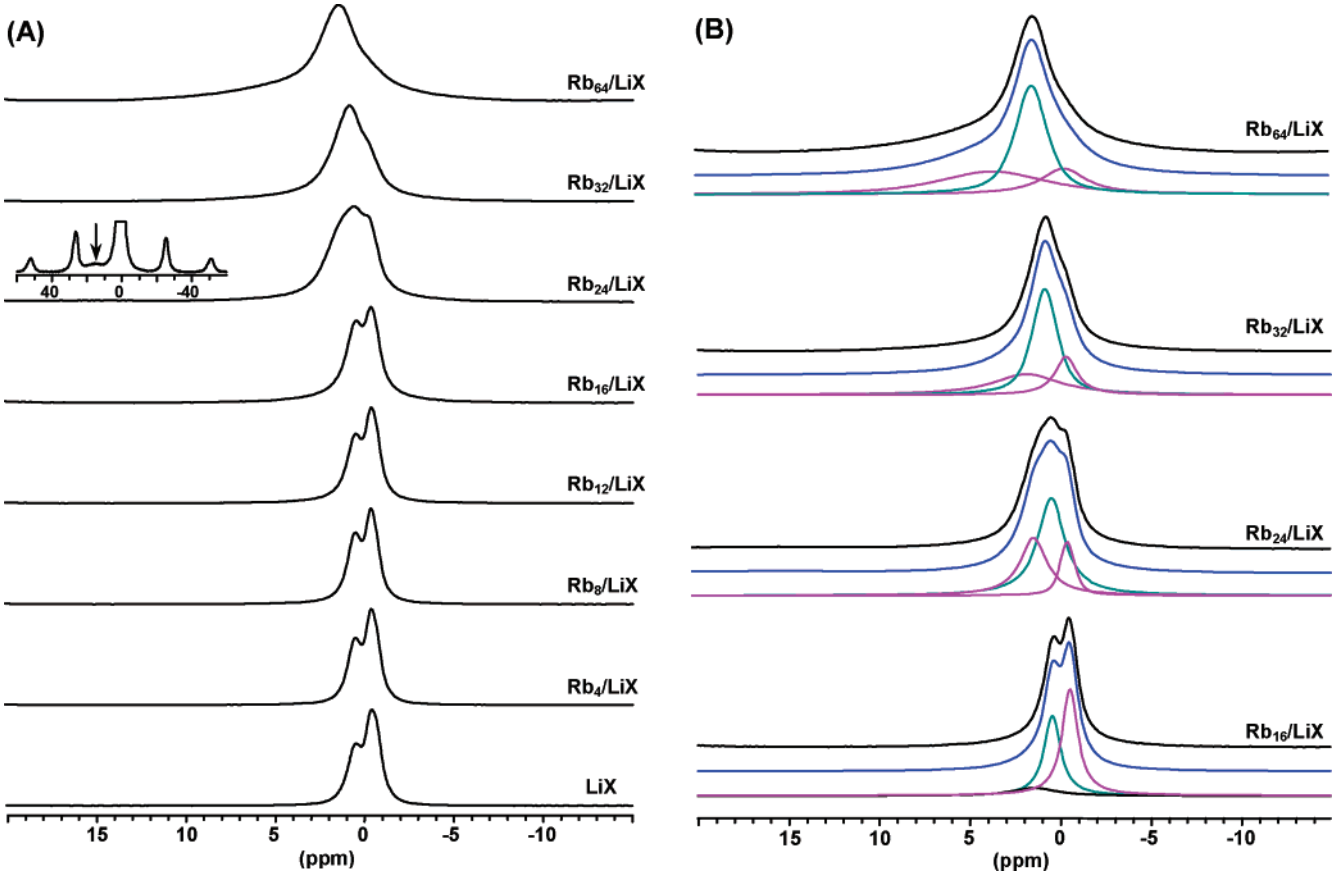


***Figure 4.*** (A) $^{7}$Li MAS NMR spectra of dehydrated Li−X zeolite and Rb-loaded Li−X samples. (B) $^{7}$Li MAS NMR spectra of the Rb-loaded Li−X samples (black) together with simulated spectra (blue) and components of the simulated spectra (color). All spectra are scaled to have the same vertical intensity.

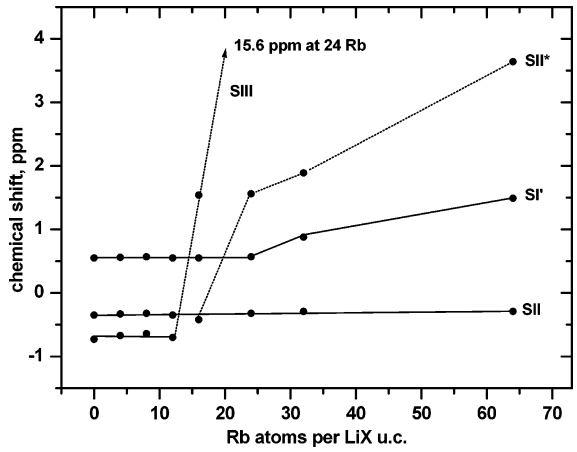


***Figure 5.*** Dependence of the $^{7}$Li NMR chemical shifts on loading in Rb/Li−X samples.

lines from SII and SII* after the split. This observation also supports the idea that SII* cations are former SII cations.

One rather important observation can be made from analysis of the $^{7}$Li SATRAS NMR spectra of the same set of Rb-loaded samples, Figure 6. The amplitude envelope of the satellite transition MAS sidebands remains practically unchanged upon introduction of rubidium, even at the highest loadings, indicating that the quadrupolar coupling parameters for the corresponding Li sites (SI′, SII) are unchanged. Consequently, it may be concluded that there are no dramatic changes in the close environment (coordination) of these cations as well. Preliminary X-ray synchrotron diffraction refinement data also indicate that lithium cations occupy SI′ and SII sites and are not displaced even at high Rb loadings.[21] Because they occupy essentially the same SI′ and SII positions in the 6-ring windows inside the sodalite and supercages, the shifts and broadening observed in the center bands are caused not by structural changes or chemical reactions, but by interactions with paramagnetic species, probably Rb atoms or clusters located inside the cages. Other paramagnetic guest species are known to cause shifts of the resonance from the SIII cations. For example, Fermi-contact shifts of SIII $Li^{+}$ were observed in the $^{7}$Li NMR spectra when oxygen was adsorbed in Li−X zeolites, which was explained by the paramagnetic properties of the oxygen molecule.[19]

There are two types of paramagnetic interactions that could influence the $^{7}$Li NMR spectra: (i) The first is the pseudocontact mechanism involving through-space dipolar interactions between nuclear and electronic moments. This affects mainly the line width, but may also cause small shifts of the lines. (ii) The second is the Fermi-contact mechanism involving through-bond interactions. The latter arises from direct transfer of the unpaired electron spin density from the paramagnetic center to the nucleus under study and results in large shifts and broadening of the NMR lines. Assuming no temperature-dependent unpairing, the magnitude of the Fermi-contact shift depends on the net electron density transferred. In the high field approximation[30]

$$\delta_{\mathrm{con}} = \frac{A_{\mathrm{N}}}{\hbar}\frac{g_{\mathrm{e}}\mu_{\mathrm{B}}S(S+1)}{3\gamma_{\mathrm{I}}kT} \qquad (1)$$

where $A_{\mathrm{N}}$ is the electron−nuclear hyperfine coupling constant.

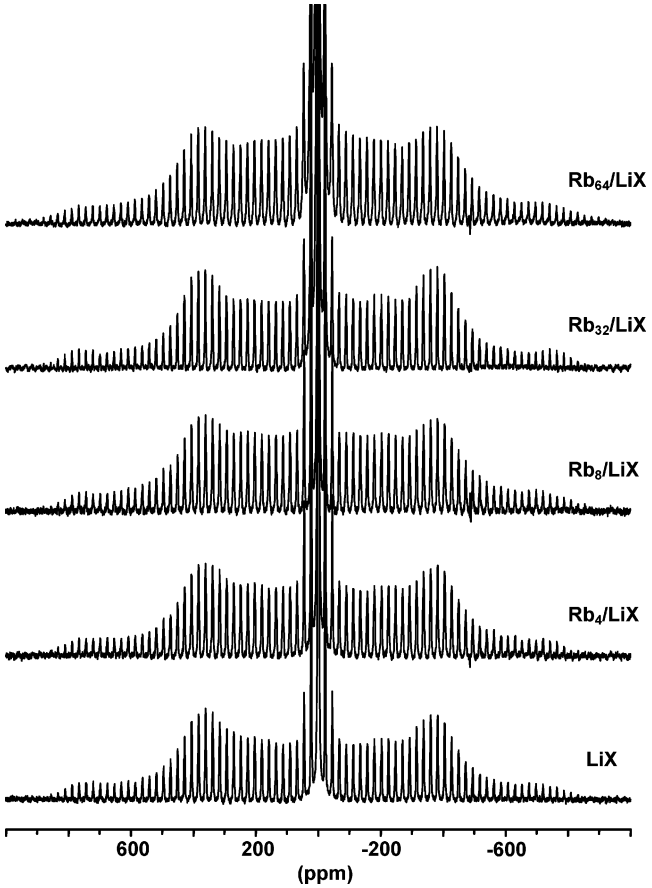


***Figure 6.*** $^{7}$Li SATRAS NMR spectra of dehydrated Li−X zeolite and Rb-loaded Li−X samples ($\nu_o$ = 155.5 MHz, $\nu_{rot}$ = 3.5 kHz).

The magnitude of $A_N$ controls the size of the shift. An important characteristic of the Fermi-contact shift is that it has an inverse temperature dependence, eq 1.

Both mechanisms can easily be recognized in the behavior of the $^{7}$Li MAS NMR spectra with Rb loading. At $x = 16$ and higher, the dramatic effects observed for the SIII $Li^+$ are characteristic of Fermi contact with a paramagnetic center. This is confirmed by variable-temperature $^{7}$Li MAS NMR experiments on $Rb_{24}$/Li−X, which show that the shift of the SIII line at 15.6 ppm has an inverse temperature dependence, Figure 7 (the corresponding spectra are shown in Figure 6s of the Supporting Information). The linear fit of the shift versus $1/T$ dependence has an intercept of 1.4 ± 0.7 ppm (at infinite $T$), which means that the Fermi-contact interaction is the major contributor to the paramagnetic shift observed. At the same time, the hyperfine coupling constant $A_N$ = 41 ± 2 kHz, obtained from the slope of the plot according to eq 1, is very small, especially when compared to the Li atomic hyperfine coupling constant $A_N$ of 379.7 MHz (for $^{7}Li^0$ in an adamantine matrix).[31] At first glance, this might be taken to indicate only weak overlap between the s orbitals of Li and Rb atoms, as much larger paramagnetic shifts (up to 1980 ppm) have been observed, for example, in the $^{7}$Li MAS NMR spectra of lithium manganate cathode materials,[32] where strong polarization transfer from $t_{2g}$ and $e_g$ orbitals of the manganese cations to Li atoms was found.

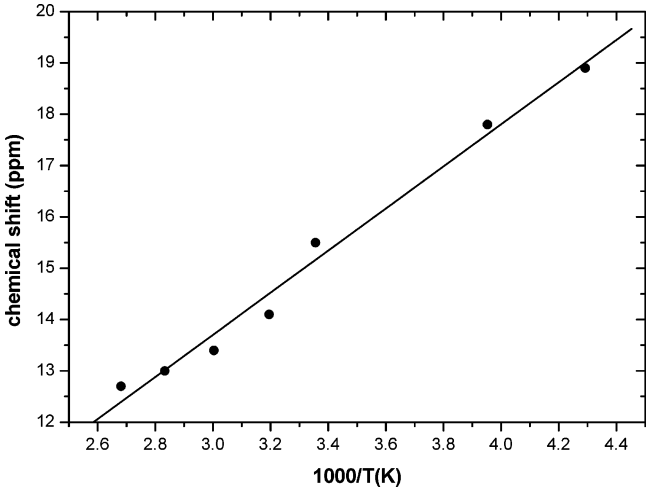


***Figure 7.*** The inverse temperature dependence of the $^{7}$Li NMR chemical shift at SIII sites in $Rb_{24}$/Li−X.

However, the behavior of the SIII line is unusual in another respect, in that although it shifts strongly above a loading of $Rb_{12}$ it shifts gradually with increasing Rb-loading. This must be a consequence of the dynamics (mentioned earlier) associated with this site. Any static $Li^+$ in Fermi contact with a paramagnetic species would be expected immediately to have a very large shift and disappear from the spectrum, whereas those not in contact should remain at the diamagnetic shift. However, if the $Li^+$ is able to exchange rapidly between SIII sites with and without contact with the paramagnetic centers, its shift will be a population weighted average of the diamagnetic and paramagnetic shifts. As Rb-loading increases, more SIII $Li^+$ will come into contact with the encroaching paramagnetic species, and the average shift will steadily increase toward the paramagnetic end.

From $x = 0$ to 12 Rb, there is no shift in the SIII signal, but there is a gradual loss of intensity (Table 2). This intensity could be lost if the $Li^+$ were displaced to some other type of site by incoming Rb, but this is unlikely as no new signal is observed in the diamagnetic shift region. The most plausible explanation is that some of the SIII $Li^+$ interact strongly with the introduced paramagnetic species to the extent that they are not only in Fermi contact with them but are also no longer dynamic, in which case they are rendered invisible. The visible signal represents the remaining exchanging SIII $Li^+$. This invisible $Li^+$ could perhaps form part of a cluster with Rb, although it is not possible to say whether it is still at the SIII site or elsewhere. Incidentally, there is a similar gradual decrease of intensity in the $^{23}$Na NMR spectra of the residual $Na^+$ (which occupy SIII sites only) in these samples. By assuming a fixed intensity for the SI′ and SII $Li^+$, the number of invisible $Li^+$ can be calculated from the values in Table 2, and this increases roughly with the number of unpaired electrons, see Table 3.

Cations in SII and SI′ sites, on the other hand, show only small paramagnetic shifts, which are likely to be of pseudo-contact origin. This is also supported by variable-temperature NMR experiments, which showed some broadening rather than shifting as the temperature decreased (Figures 5s and 7s of the Supporting Information).

The difference in the shift mechanisms for the different types of Li cations can be related to the local structure at each type of site and leads to the conclusion that most, if not all, of the

(30) Aime, S.; Bertini, I.; Luchinat, C. *Coord. Chem. Rev.* **1996**, *150*, 29.
(31) Jones, R.; Howard, J. A.; Joly, H. A.; Edwards, P. P.; Singer, R. J. *Magn. Reson. Chem.* **1995**, *33*, S98.
(32) Lee, Y. J.; Wang, F.; Grey, C. P. *J. Am. Chem. Soc.* **1998**, *120*, 12601.

***Table 3.*** Numbers of NMR-Invisible $^7$Li Cations and Unpaired Electrons per Unit Cell

| Rb loading *x* | invisible Li/uc | unpaired electrons/uc |
|---|---|---|
| 0 | 0 | 0 |
| 4 | 3.1 | 2.6 |
| 8 | 6.0 | 4.2 |
| 12 | 6.0 | 6.2 |
| 16 | 10.4 | 7.0 |
| 24 | 15.8 | 13.4 |
| 32 | 18.5 | 13.1 |
| 64 | 18.5 | 10.9 |

paramagnetic centers are present in the supercages and not in the sodalite cages. (This is a significant observation, because in many related non-lithium systems the sodalite cages usually do contain paramagnetic centers.) There are several strong arguments for this. The cations at site SIII inside the supercage (Figure 2) are poorly coordinated and are exposed to close contact with incoming guest species. Thus, paramagnetic rubidium-containing species formed inside the supercage can make direct contact with the SIII cations, so that electron transfer via the Fermi-contact mechanism is possible. On the other hand, lithium cations at sites SI′, SII, and SII* must be much more effectively shielded from direct contact with the paramagnetic species by neighboring framework atoms.

Several things argue against paramagnetic centers being located inside the sodalite cages: (a) Although paramagnetic centers have been found in the sodalite cages in analogous non-lithium systems, for example, $Na_4^{3+}$, $K_4^{3+}$, $K_3^{2+}$, etc., in alkali metal-loaded zeolites X,Y and sodalite,[1,3,5,12,13] these are essentially trapped electron species, which show characteristic ESR multiplets due to hyperfine interactions of the unpaired electron with the surrounding cations. At the same time, the NMR resonances of these cations are strongly paramagnetically shifted and in practice cannot be detected. Similarly, in the present case, if the SI′ and SII $Li^+$ cations were in close Fermi contact with a paramagnetic center located inside the sodalite cage, then their NMR signals should be very strongly shifted. Hence, as the number of paramagnetic species in the sodalite cages increases, the diamagnetic NMR signals of $Li^+$ at these sites should lose intensity, which is not observed. (b) Assuming that the $Li^+$ cations remain in the 6-rings, the only paramagnetic species other than a trapped electron (which is excluded by point (a) above) which could fit into the sodalite cage are $Rb^0$ and $Na^0$ (the latter from the residual $Na^+$ present in the starting material). Most likely, these would have Fermi contact with the $Li^+$, but even if they did not they should still display their own hyperfine interaction in the ESR spectra, and this has not been detected either. Note that the sodalite cage center to $Li^+$ distances are 3.39 Å for SI′ and 4.17 Å for SII, respectively, and thus it is just possible to fit in a single $Rb^0$ ($r = 2.48$ Å) without van der Waals overlap with the $Li^+$ ($r = 0.78$ Å). In any case, there is no reported example of an ESR spectrum attributed to an alkali metal $M^0$ species in zeolites. The claims for $M^0$ mentioned in the Introduction are all derived from crystallographic data. (c) Also note that a situation with paramagnetic centers in the sodalite cages and none in the supercages can be ruled out, because SIII would then be the most distant site and Fermi contact with it would not be possible.

It then remains for us to examine the different behavior of the resonances for the SI′, SII, and SII* sites. The pseudocontact electron−nucleus dipolar interaction has a $1/r^3$ dependence on the distance $r$ between the nucleus and the paramagnetic center, but the additive effect of all paramagnetic centers in reasonable proximity to the $Li^+$ must also be taken into consideration. Thus, SII* must be significantly closer to a paramagnetic center than SII and SI′ to show the strongest effects. Two plausible scenarios can be envisaged: (1) The SII* and SII site resonances could depend on the presence or absence, respectively, of paramagnetic centers in the supercage. The observation that the $Li^+$ at SI′ show slightly stronger shifting than those at SII may relate to the number of supercages (which can potentially contain paramagnetic centers) adjacent to them: SI′ has six neighboring supercages, whereas SII in the face of a "diamagnetic" supercage has only three other neighboring supercages and hence potentially fewer paramagnetic centers with which to interact. The relatively constant intensity ratio of these two resonances may then be related to the observation that for $x = 24$ Rb and above the number of unpaired electrons does not change much, see Table 3. (2) Alternatively, SII* and SII might be distinguished by their relative proximity to the paramagnetic center within the same supercage. At low loading, the unpaired electron has to be located sufficiently distant from all of the SII's that the interaction is weak, then at higher loading it must be brought much closer to some SII (which then become SII*) than others (and SI′). The $1/r^3$ dependence for interaction at 2 Å distance versus 7 Å is a factor of ~43, or for 3 Å versus 7 Å is ~13, so the magnitude of the effects can have a lot to do with where the unpaired electron is in the cage. The paramagnetic contents of the cages must be qualitatively different at different loading levels, and the growth of clusters will likely cause a redistribution of the unpaired electrons. Because of increased cluster size, or shift in location, the unpaired electrons must at some point start to interact more strongly with other Li.

Thus, it can be seen that the behavior of $^7$Li NMR signals may be used as an indicator of the location and distribution of paramagnetic Rb clusters within the zeolite pores. Similar but less detailed information has previously been obtained from $^{27}$Al and $^{29}$Si NMR spectra of alkali metal-loaded zeolite A.[33]

**Na-, K-, and Cs-Loaded Zeolite Li−X.** Samples of Li−X zeolite loaded with Na, K, and Cs to the extent of $x = 4$, 12, 32 per unit cell were also synthesized and studied. $^7$Li MAS and SATRAS NMR spectra measured for these samples are very similar to the samples loaded with Rb (Figures 1s, 2s, 3s, 4s of the Supporting Information), indicating common behavior for all, although the paramagnetic effects for Na-loaded samples are less pronounced than those for the other alkali metals (Figure 8). This may be due to the smaller size of Na, which will mean less crowding of the atoms and hence a greater distance for the interaction between Li nuclei and unpaired electrons.

**Alkali Metal-Loaded Zeolite Li−A.** Zeolite A (LTA structure type)[22] also consists of sodalite units, but these are now connected via four-membered double rings to form a cubic structure with large α-cages. In dehydrated Li−A zeolite, Li cations have been found at three different sites.[19c,34] The site SI (adopting the same labeling scheme as was used in refs 19c, 34) is in the 6-ring windows connecting sodalite and α-cages. There are 64 such sites per unit cell, and they are fully occupied

(33) Moran, K. L.; Barker, P. D.; Readman, J. E.; Edwards, P. P.; Dupree, R.; Anderson, P. A. *Chem. Commun.* **2000**, 55.
(34) Porcher, F.; Souhassou, M.; Dusausoy, Y.; Lecomte, C. *C. R. Acad. Sci. Paris II* **1998**, *1*, 701.

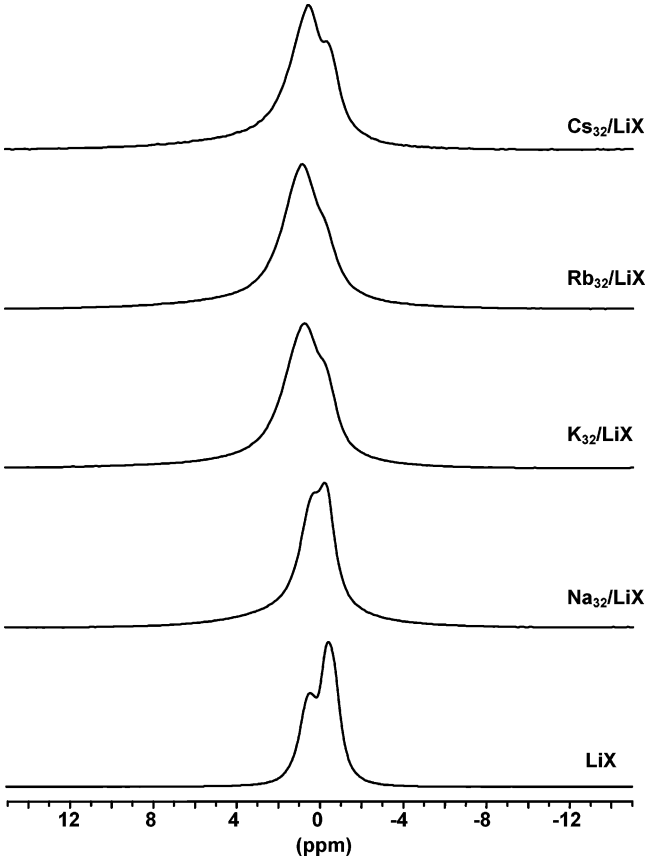


***Figure 8.*** $^{7}$Li MAS NMR spectra of dehydrated Li−X zeolite and $M_{32}$/Li−X samples (M = Na, K, Rb, Cs).

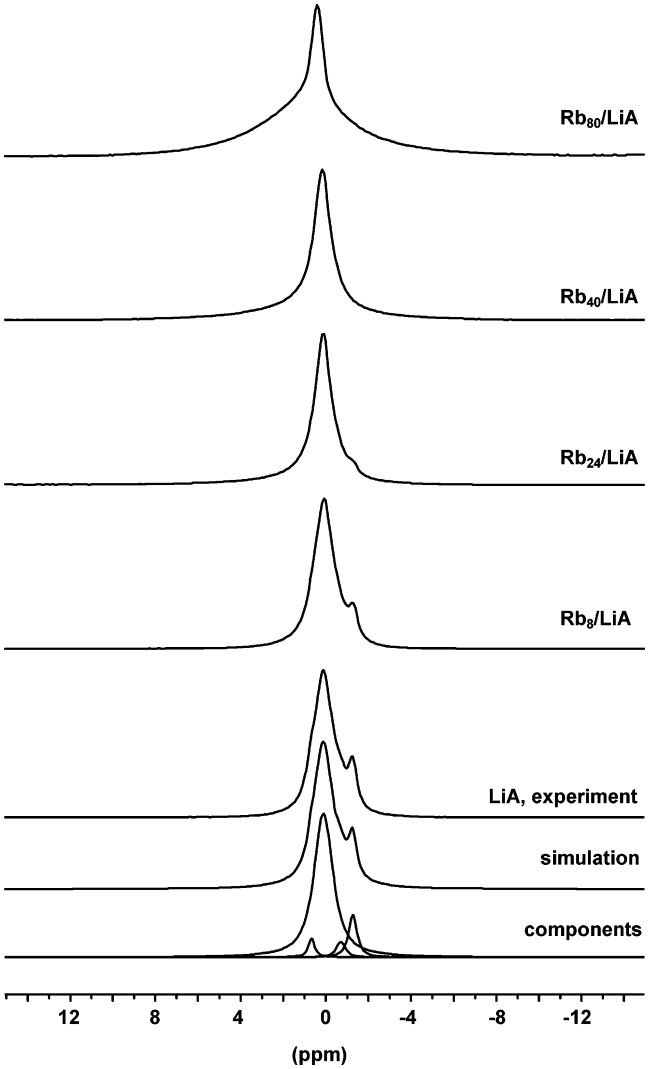


***Figure 9.*** $^{7}$Li MAS NMR spectra of dehydrated Li−A zeolite (shown with deconvolution) and Rb-loaded Li−A samples. All spectra are scaled to have the same vertical intensity.

with Li cations. The remaining 26 $Li^+$ and 6 $Na^+$ cations of the material studied here are then distributed among SII and SIII sites. Site SII cations occupy the 8-ring windows connecting α-cages. If only one cation occupies the window, there are 24 such sites per unit cell. Site SIII cations are located inside the α-cages in front of 4-ring windows. Although there are 96 SIII sites per unit cell, very few are actually occupied. Unfortunately, for Li−A, the assignment of the $^{7}$Li MAS NMR lines to particular crystallographic sites is not as straightforward as in Li−X. Simulation of the spectra required at least four components, as shown in Figure 9. The most intense line, at +0.1 ppm, can be attributed to lithium cations at SI sites because these have the highest population. The relatively isolated line shifted to high field, at −1.3 ppm, is likely due to cations at SIII sites, which, like the exposed SIII sites of Li−X, show specific behavior under oxygen adsorption.[19c] The remaining two lower intensity lines, at +0.7 and −0.7 ppm, must then be attributed to Li cations in 8-ring windows, possibly singly and doubly occupied,[34] and/or perhaps dependent on the distribution of $Na^+$ nearby.

The lithium cations at the SIII sites are the first to experience the effects of the paramagnetic species formed upon Rb loading. The line gradually disappears with increasing loading, and the logical explanation is that those SIII cations in cages containing a paramagnetic center are shifted out of the spectrum through Fermi contact. A similar process may occur for the SII cations, which must be relatively exposed to close contact with the paramagnetic centers, but unfortunately due to the overlapping of peaks, it is not possible to trace every single component separately, and it is not clear whether there is intensity diminution because of Fermi contact shifts or just strong broadening.

Line-broadening with small shifts for some of the SI cations is also obvious at high loading, apparently of pseudocontact origin. In fact, for $Rb_{80}$/Li−A, the site SI cation resonance has two components; one, which has about 25% of the total intensity, has a very slight shift (0.30 ppm downfield) but no significant broadening as compared to Li−A (line widths ∼150 Hz), while the other is shifted further (0.91 ppm downfield) and is substantially broader (∼770 Hz). It is significant that, even at these highest loadings, a considerable number of the SI cations retain NMR parameters similar to the starting material (including the $C_Q$ as seen in the SATRAS ssb pattern, see Figure 10s of the Supporting Information). This could mean either (a) that paramagnetic clusters are not formed in every α-cage throughout the sample, or (b) that the paramagnetic center is significantly closer to some SI sites than others within the α-cage.

The retention of most of the SI cation intensity as the Rb-loading increases once again suggests either that there are very few (if any) paramagnetic centers inside the sodalite cage or

that, if present, they do not have Fermi contact with the $Li^+$. Note that there is slightly more room in this cage than there is in the Li−X sodalite cage, because all eight $Li^+$ are at 3.84 Å from the cage center, but the same counterarguments apply regarding trapped electrons or $M^0$ centers as were discussed for Li−X.

$^7$Li NMR results for zeolite Li−A, loaded with Na, K, and Cs, resemble very much those obtained for Rb-loaded Li−A zeolite (spectra 8s and 9s of the Supporting Information).

## General Discussion and Conclusions

The $^7$Li NMR results presented here provide essential information about the local environments of Li cations in Li−X and Li−A zeolites loaded with alkali metals. Not only can the crystallographically different Li sites be resolved in both starting and loaded zeolites, but also changes involving Li at these sites can be followed as a function of loading. The different location of each type of $Li^+$ means that they experience different effects when alkali metals are introduced. Site SIII cations in both Li−X and Li−A, and the SII sites of Li−A, are in relatively exposed positions in the large cages of their respective frameworks. The NMR resonances of Li cations at these sites are the first to show the presence of paramagnetic clusters inside these cavities as the metal loading increases. At low loadings, paramagnetic clusters located in the large cages cause strong paramagnetic shifts and broadening of the NMR line from cations at these sites, via the Fermi-contact mechanism. Similar observations have been made while studying oxygen adsorption on Li−X, Li−A,[19] and Na−X[35] zeolites. The formation of paramagnetic species has been clearly demonstrated in our ESR experiments on these systems.[21] Depending on the specific alkali metal and its loading, several types of paramagnetic clusters have previously been observed and identified. Unfortunately, ESR does not provide direct information on their location in the zeolite, so that additional structural studies are needed. As demonstrated in this paper, however, $^7$Li NMR data can provide important information on this subject.

Cations located at sites SI′ and SII in zeolite Li−X, and SI in zeolite Li−A, are effectively shielded from direct interaction with paramagnetic centers by atoms of the zeolite framework. The key point here is the coordination of the Li cations in the 6-ring sites, which is much fuller than in the other sites. Such cations experience weak through-space interactions with the paramagnetic species when the concentration of the latter increases. It is interesting that cations at site SI′ inside the sodalite cages are only moderately affected, while stronger paramagnetic effects are observed for SII* sites at the interface with the supercages. The latter would be much more exposed to paramagnetic centers in the supercages than those in SI′. It follows that, in contrast with many other alkali metal-loaded zeolite systems where $Li^+$ is not the cation,[5] the paramagnetic species in Li−X and Li−A zeolites are found mainly in the large cages and not within the sodalite cages.

Another important observation is the apparent inertness of $Li^+$ cations in these zeolites toward reduction by the incoming heavier alkali metals, as can be seen in the SATRAS spectra in particular. This is even more intriguing when one considers that the gas-phase enthalpies for electron transfer seem to favor reduction of $Li^+$ by all of the other alkali metals $Na^0$, $K^0$, $Rb^0$, and $Cs^0$ (Table 4).[36] While reaction should occur for the $Li^+/M^0$ pair in isolation, it is clear that in the zeolite other factors involving these systems as a whole come into play. In this regard, it is useful to consider another trend: a comparison of the stabilities of alkali metal oxides reveals that the oxides of lithium are more stable than other alkali metal oxides (Table 4),[37] an indication of the high oxygen affinity of lithium.

***Table 4.*** Ionization Enthalpies of the Alkali Metals (kJ/mol)[36] and Standard Enthalpies of Formation of the Alkali Metal Oxides, $\Delta H°_{f,298K}$ (kJ/mol);[37] the Most Common Oxides Are Italicized

| M | Li | Na | K | Rb | Cs |
|---|---|---|---|---|---|
| $M^+$ | 520.1 | 495.7 | 418.7 | 402.9 | 375.6 |
| $M_2O$ | *−599.6* | *−416.5* | −362.0 | −331.0 | −318.4 |
| $M_2O_2$ | *−633.5* | *−505.3* | *−494.4* | *−426.1* | *−403.1* |
| $MO_2$ | N/a | −260.2 | *−283.2* | *−288.3* | *−295.4* |

The same trend might well be expected in zeolites, with the Li-forms of zeolites being the most stable, but, unfortunately, the standard enthalpies of formation of the zeolites themselves in their various ionic forms are largely unknown. Similar conclusions about the "inertness" of lithium in this context, although supported by indirect observations, were drawn when Li−X zeolites loaded with alkali metals were first studied with ESR spectroscopy.[12,13] Earlier quantum-chemical calculations showed that the residual charge on Li cations in the 6-ring was less than one-sixth of that on a sodium ion in a similar site, and less than one-tenth of that on a potassium ion.[38]

Another aspect of this perhaps is the apparent absence of the paramagnetic species $Li_4^{3+}$ in the sodalite cages. $Na_4^{3+}$ in particular seems to occur readily and may be regarded as a trapped electron species, where the $e^-$ interacts with four $Na^+$ cations already present inside the cage. Indeed, whether a similar species could be formed with Li in place of Na or whether the strong interaction of Li with the framework O atoms would prevent it from doing so would make an interesting theoretical study. It is likely that the reduced positive charge on the Li "cations" mentioned above[38] prevents the sodalite cage from being a good trapping site.

With their apparent resistance to reduction, the Li-forms of zeolites provide a unique porous matrix to accommodate unusual species formed by incoming alkali metal guests. Recently, the first experimental (NMR) evidence suggesting the formation of rubidide, $Rb^-$, and potasside, $K^-$, species in Li−A zeolite was reported.[11] Preliminary neutron and X-ray powder diffraction measurements on $Rb_{24}$/Li−A suggest that there is a Rb atom or ion at or near the center of about 70% of the sodalite cages, a highly symmetric site, surrounded by 8 $Li^+$ in the 6-ring windows.[21] The formation of these and other unusual species in the cages of zeolites such as X and A are currently under study. In all of these cases, the $Li^+$ cations may act as "inert" solvent species, whose role is to facilitate cluster formation, and stabilize the resulting clusters, without strong involvement in chemical interactions with the guest. It is possible that unusual species incorporating guest substances other than alkali metals could also be formed in the Li-forms of zeolites, opening up exciting new research opportunities.

(35) Accardi, R. J.; Lobo, R. F.; Kalwei, M. *J. Phys. Chem. B* **2001**, *105*, 5883.
(36) Cotton, F. A.; Wilkinson, G. *Advanced Inorganic Chemistry*, 5th ed.; John Wiley & Sons: New York, 1988.
(37) Hart, W. A.; Beumel, O. F.; Whaley, T. P. *The Chemistry of Lithium, Sodium, Potassium, Rubidium, Cesium and Francium, Comprehensive Inorganic Chemistry*; Pergamon Press: Elmsford, NY, 1973; Vol. 13.
(38) Beran, S. *J. Phys. Chem. Solids* **1982**, *43*, 221.

Despite the valuable information obtained from $^{7}$Li MAS NMR, a number of questions still remain: for instance, while the ESR and NMR results indicate that several different paramagnetic species can exist in any one sample, and that they may change with increasing alkali metal loading,[21] the precise nature of these remains unknown. Where exactly are they located with respect to the centers of the cages? Further work is now in progress to address these questions.

In conclusion, the comparative inertness of Li cations in zeolites makes the Li-exchanged forms of zeolites excellent porous substrates for the containment of unusual chemical species. $^{7}$Li MAS NMR has been shown to be very sensitive to the presence of intrapore alkali metal clusters in Li−X and Li−A zeolites. This acute sensitivity can be used to locate such species inside the zeolite framework and to follow their evolution with metal loading.

**Acknowledgment.** This work was supported by a Cooperative Research Project Grant from the National Research Council Canada − British Council Science and Technology Fund. The authors thank Victor Boyko (NRC) for the elemental analyses.

**Supporting Information Available:** $^{7}$Li MAS NMR spectra of Li−X and Li−A zeolites loaded with alkali metals and recorded at room and variable temperatures. This material is available free of charge via the Internet at http://pubs.acs.org.

JA0491580